Intermediate- and short-range order in phosphorus-selenium glasses

Aleksei Bytchkov,[1,*] Mariana Miloshova,[2] Eugene Bychkov,[2] Shinji Kohara,[3] Louis Hennet,[1] and David L. Price[1]

[1]*Conditions Extrêmes et Matériaux: Haute Température et Irradiation and Université d'Orléans, 1d Avenue de la Recherche Scientifique, F-45071 Orléans Cedex 2, France*

[2]*Université du Littoral, F-59140 Dunkerque, France*

[3]*Japan Synchrotron Radiation Research Institute, 1-1-1 Kouto, Sayo-cho, Sayo-gun, Hyogo 679-5198, Japan*

(Received 15 December 2010; published 4 April 2011)

State-of-the-art neutron and x-ray diffraction measurements have been performed to provide a definitive picture of the intermediate- and short-range structures of P_xSe_{1-x} glasses spanning two glass regions, $x = 0.025$–0.54 and 0.64–0.84. Liquid P_4Se_3 and amorphous red P and Se were also measured. Detailed information was obtained about the development with increasing phosphorous concentration of intermediate-range order on the length scale ∼6 Å, based on the behavior of the first sharp diffraction peak. Attention is also paid to the feature in the structure factor at 7.5 $Å^{-1}$, identified in earlier numerical simulations, provides further evidence of the existence of molecular units. The real-space transforms yield a reliable statistical picture of the changing short-range order as x increases, using the information about types and concentrations of local structural units provided by previous NMR measurements to interpret the trends observed.

DOI: 10.1103/PhysRevB.83.144201 PACS number(s): 61.43.Fs, 61.05.cp, 61.05.fm, 81.05.Kf

I. INTRODUCTION

A renewed interest in binary chalcogenide glasses has recently developed owing to their applications in infrared detectors, lenses, optical fibers, and nonvolatile memories. The phosphorus-selenium system P_xSe_{1-x} exhibits the widest glass region among known binary chalcogenide systems,[1] covering almost the entire composition range from $x = 0$ to 1, and red phosphorus ($x = 1$) is usually also amorphous. A small gap centered at the crystalline composition $x = 4/7$ separates two glass-forming regions, Se rich with $x = 0$–0.54 and P rich with $x = 0.6$–1.

Earlier studies of the Se-rich glass region identified several local structural units whose concentrations depend on composition. However, there were significant disagreements about the nature of the units present. The authors of neutron diffraction, extended x-ray-absorption fine structure (EXAFS), and Raman measurements,[2,3] by analogy with known crystal structures in the P_xSe_{1-x} and P_xS_{1-x} systems, proposed a model of PSe_n units embedded in a Se matrix for the range $x = 0.25$–0.5; subsequent density functional theory[4] and *ab initio* molecular dynamics (AIMD) simulations[5] supported the presence of PSe_n units at $x = 0.5$. On the other hand, magic angle spinning NMR (MAS-NMR),[6,7] and Raman[8] measurements were interpreted in terms of $Se = PSe_{3/2}$ tetrahedra, $PSe_{3/2}$ pyramids, and $Se_{2/2}P\text{-}PSe_{2/2}$ ethylenelike units, the latter dominating at higher P concentrations, $x = 0.4$–0.5.

There was also disagreement about the P-rich glass region, although less information was available. The authors of neutron diffraction and inelastic scattering experiments[9,10] at $x = 0.67$ proposed units made up of two P_4Se_3 molecules joined by two P atoms at their bases. On the other hand, Raman scattering measurements in the range $x = 0.75$–0.84 were interpreted on the basis of P_4Se_3 units embedded in a matrix of red P.[11]

Recently, a comprehensive study of eight glasses with compositions extending over both the Se- and P-rich glass regions, together with crystalline α- and β-crystalline P_4Se_3 and crystalline violet and amorphous red P as references, was carried out using two-dimensional (2D) ^{31}P homonuclear through-bond correlation and *J*-resolved MAS–NMR.[12] Several types of structural units were identified, shown in Fig. 1. The results showed that the most Se-rich glasses are composed of $Se = PSe_{3/2}$ tetrahedra (labeled P4 in Fig. 1) linked together by Se-Se chains; at intermediate compositions one finds a mixture of tetrahedral and original $PSe_{3/2}$ units (P3) with ethylenelike $Se_{2/2}P\text{-}PSe_{2/2}$ motifs (P2) appearing as x increases; and finally, approaching the gap between the two regions, the glasses are composed of P_4Se_3 cage molecules (P1) embedded in a $Se_{2/2}P\text{-}PSe_{2/2}$ polymeric network. The relative concentrations of all four units, and by inference those of the Se-Se chains, was established over the range $x = 0.025$–0.54. In the P-rich region, the glass at $x = 0.67$ consists of P_4Se_3 units embedded in a red-P matrix (P0); as x increases further, the concentration of P_4Se_3 units decreases while that of the red-P matrix increases, together with that of other molecular units that may include P_4Se_2 (not shown), obtained from P_4Se_3 by removing the Se from one P-Se-P bond.

To complement this comprehensive information on the types and concentrations of local structural units, the present work aimed to obtain state-of-the-art neutron and x-ray diffraction data to provide a definitive picture of the short- and intermediate-range structures of P-Se glasses spanning both glass regions. Specific goals were as follows: (1) to obtain detailed information about the development with increasing P concentration of intermediate-range order on the length scale ∼10 Å, based on the behavior of the first sharp diffraction peak (FSDP); and (2) to obtain a reliable statistical picture of the short-range order, using the information about types and concentrations of local structural units provided by the NMR measurements to interpret the trends observed as the P concentration increases. Attention is also paid to the feature in the structure factor at 7.5 $Å^{-1}$, identified in AIMD simulations[5] as a signature of molecular units. Measurements were made

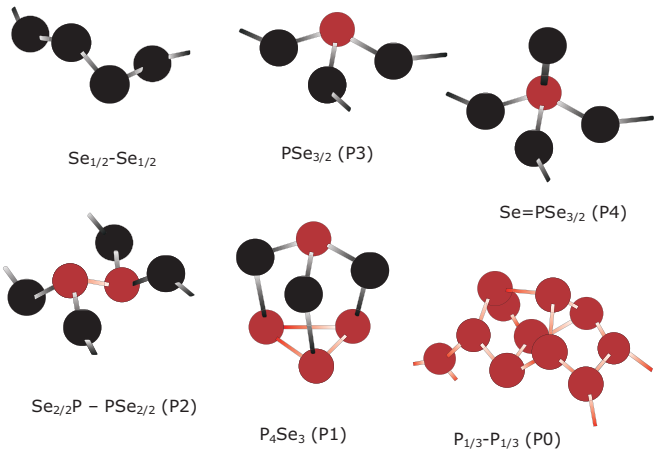

FIG. 1. (Color online) Structural units in P-Se glasses identified by solid-state NMR experiments (Ref. 12).

on many glasses spanning both concentration regions and also on liquid P_4Se_3 and amorphous red P.

II. EXPERIMENTAL

Details of sample preparation and measurements of density and glass transition temperatures T_g can be found in Ref. 12, and the results are given in the electronic supplementary information for Ref. 12. Neutron diffraction measurements were carried out using SANDALS diffractometer[13] at the ISIS spallation neutron source (Rutherford-Appleton Laboratory, UK). This instrument provides diffraction data over an extended range in reciprocal space (values of scattering vector Q up to 50 Å^{-1}), leading to high resolution in real space. High-energy x-ray diffraction measurements were conducted at several synchrotron beam lines: 11-ID-C at APS (Argonne National Laboratory, IL, USA),[14] ID15 at ESRF (France),[15] and BL04B2 at SPring-8 (Japan).[16] The x-ray energies were 115 keV at APS, 90 keV at ESRF, and 62 keV at SPring-8, providing data at Q values up to 30 Å^{-1}. At ESRF a 2D setup was used with a MAR345 image plate, whereas at APS and SPring-8 the measurements were made in a one-dimensional (1D) scanning mode with a Ge detector. All measurements were made at room temperature, except for the measurements at ID15 in the liquid at $x = 4/7$ that covered the range 543–663 K. The diffraction data were reduced with standard procedures.[16,17]

III. RESULTS

A. Reciprocal space

Weighted average structure factors $S(Q)$ were derived from the measured scattering cross section per atom $d\sigma/d\Omega$ through the relation

$$\frac{d\sigma}{d\Omega} = \left|\sum_a c_a \bar{b}_a\right|^2 [S(Q) - 1] + \sum_a c_a \overline{b_a^2}, \qquad (1)$$

in the case of neutron scattering, where c_a, $\bar{b}_a$, and $\overline{b_a^2}$ are, respectively, the atomic concentration, average (over isotopes and spin states) of the neutron-nucleus scattering length, and mean-square scattering length of element a. In the x-ray case, b_a in Eq. (1) is replaced by $f_a(Q)$, the atomic scattering factor of element a. The $S(Q)$'s measured by neutrons and x rays are quite similar because the ratios of scattering lengths and form factors for P and Se are not very different: $\bar{b}_{Se}/\bar{b}_P = 1.6$, $f_{Se}(0)/f_P(0) = 2.3$.

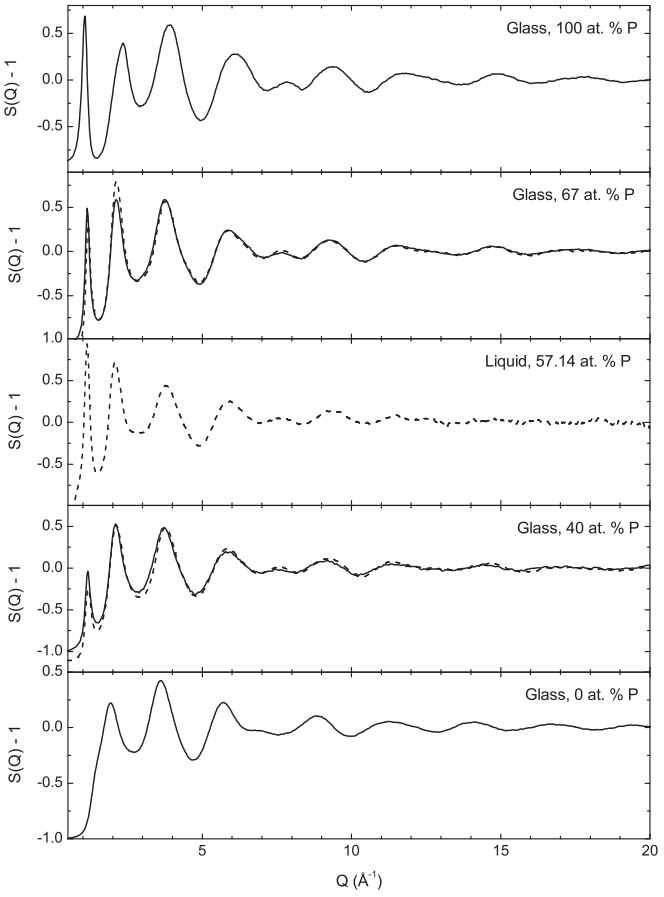

FIG. 2. Structure factors of P, $P_{0.67}Se_{0.33}$, $P_{0.4}Se_{0.6}$, and Se glasses and liquid P_4Se_3. Neutron results: solid lines; x-ray results: dotted lines.

Results for $S(Q)$ for some selected compositions are shown in Fig. 2. They exhibit distinct oscillations up to 30–35 Å^{-1} and change systematically with x. The neutron $S(Q)$'s are similar to those reported in the literature.[2,3,10]

The most remarkable changes are observed for the FSDP in the region $Q = 1$–1.5 Å^{-1}. This is a characteristic signature of intermediate-range order in disordered materials.[18,19] In order to extract the parameters of the FSDP, a parabolic function was used to approximate the background underneath it, allowing the FSDP to be isolated and fitted with a Gaussian or Lorentzian. Neither function fitted the exact shape of the most intense FSDPs, but the former was significantly better for the less intense peaks and was therefore used for all the compositions.

The amplitude A_1, width W_1, and position Q_1 of the FSDP are shown as a function of composition in Fig. 3. The fitting procedure just described gives a small positive amplitude for pure Se, corresponding to the slight shoulder that can be seen in Fig. 2. As x increases, the amplitude increases 15-fold to the end of the first glass region at $x = 0.5$, drops slightly at the beginning of the second glass region at $x = 0.64$,

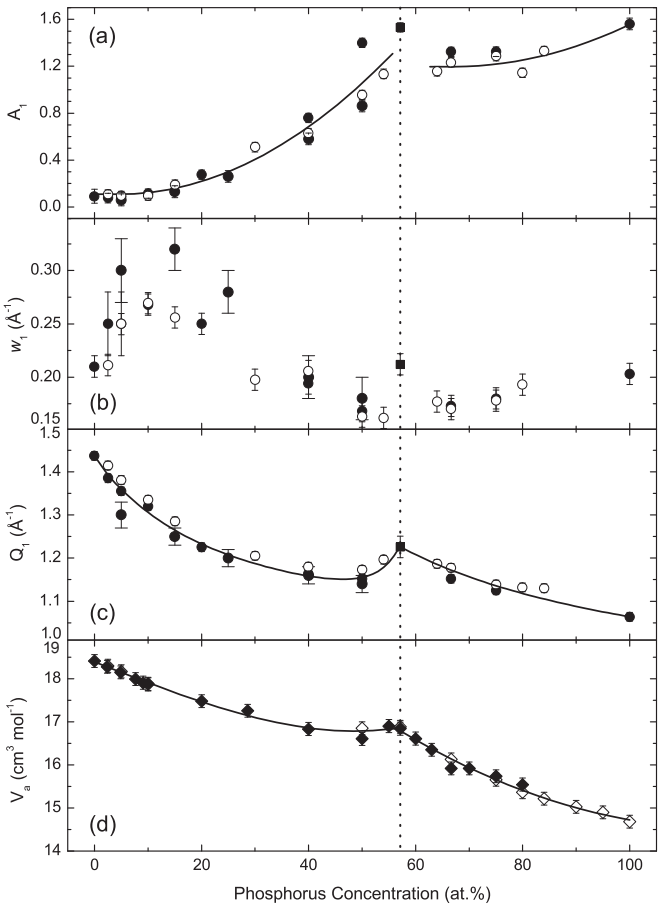

FIG. 3. (a) Amplitude A_1, (b) full width at half maximum w_1, and (c) position Q_1 of the first sharp diffraction peak in P-Se glasses obtained from Gaussian fits: neutron results, •; x-ray results, ○; liquid P_4Se_3, ■. (d) Atomic volume V_a of P-Se glasses: Ref. 12, ♦; Ref. 1, ◇. The solid lines are a guide to the eye, and the dotted line indicates the P_4Se_3 composition.

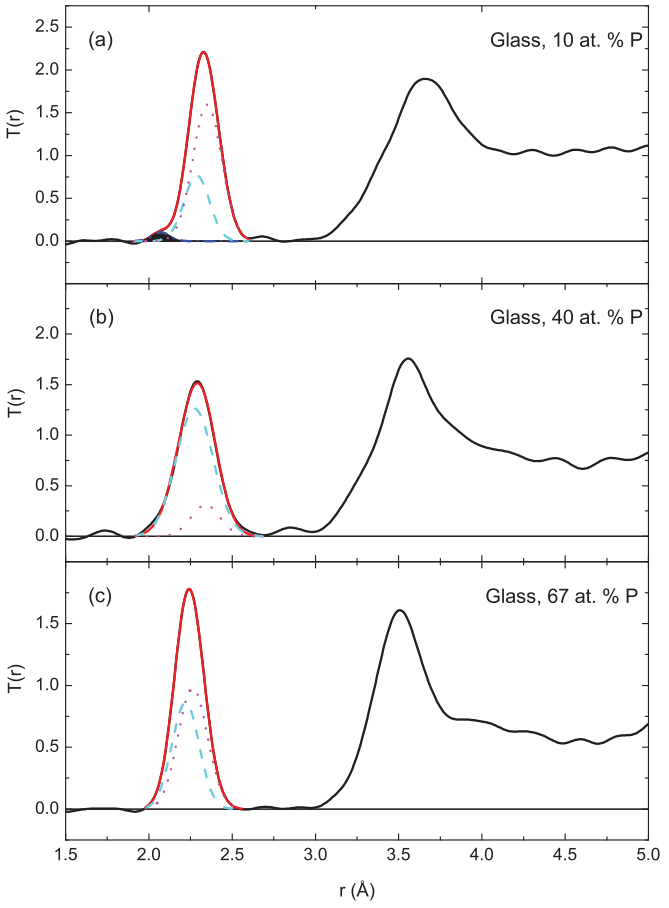

FIG. 4. (Color online) Total correlation functions for three P-Se glasses; the glass with 10 at. % P is fitted with three Gaussians, and those with 40 and 67 at. % P with two Gaussians, using the procedures described in the text: single-bond P-Se and P-P correlations, cyan dashed lines; Se-Se correlations, magenta dotted lines; double-bond P = Se correlations, blue dashed-dotted line with filled area under the peak; total correlations, red solid lines.

and then increases again toward pure *a*-P. The width has a nonmonotonic variation with x, exhibiting a broad maximum at approximately $x = 0.1$ and a broad minimum around the P_4Se_3 composition ($x = 0.57$). The position shows an overall decreasing trend with increasing x, with a cusp around the P_4Se_3 composition. The atomic volume, shown in the lowest panel of Fig. 3, shows a remarkably similar behavior. The reasons for this apparently contradictory behavior will be discussed in the next section.

The FSDP for liquid P_4Se_3, separating the two glass regions, has an amplitude and width slightly higher than the neighboring glasses. Its position, measured at 543 K, was extrapolated to room temperature, taking into account the thermal shift, $\partial Q_1/\partial T = -2.6 \times 10^{-4}$ Å^{-1}K^{-1}, measured over the 543–663 K range; the extrapolated value is consistent with those of the neighboring glasses.

The second and third peaks in the P-Se glasses correspond to chemical and topological short-range order, respectively;[19] the second peak tends to increase in intensity toward the equiatomic composition, while the third peak exhibits relatively small variations with composition and occurs near $5\pi/2r_1$, where r_1 is the mean nearest-neighbor distance. The remaining interesting feature is the small peak near 7.5 Å^{-1} that is absent at low x, starts to appear at $x = 0.2$, is fully developed at $x = 0.3$, and remains almost unchanged up to pure P.

B. Real space

Total correlation functions $T(r)$ were derived through the usual Fourier transform,

$$T(r) = 4\pi\rho_0 r + \frac{2}{\pi}\int_0^{Q_{\max}} Q[S(Q) - 1]\sin Qr\, M(Q) dQ, \quad (2)$$

where ρ_0 is the total number density, $M(Q)$ is the Lorch modification function,[20] and $Q_{\max}$ was taken as 30 Å^{-1} for the glasses and as 20 Å^{-1} for liquid P_4Se_3. Results for some selected compositions are shown in Fig. 4.

The $T(r)$'s defined in Eq. (2) are weighted averages of partial total correlation functions for the different atom pairs (*a*,*b*):

$$T(r) = \sum_{ab} W_{ab} T_{ab}(r) = \sum_{ab} c_a c_b \frac{\bar{b}_a \bar{b}_b}{\left|\sum_a c_a \bar{b}_a\right|^2} T_{ab}(r). \quad (3)$$

The first peak in the region $r = 2.0$–2.5 Å corresponds to a combination of P-P, P-Se, and Se-Se nearest-neighbor

correlations, depending on composition. In trigonal Se the Se-Se nearest-neighbor distance is 2.37 Å,[21] in crystalline P_4Se_5 the mean P = Se, P-Se, and P-P bond lengths are 2.12, 2.26, and 2.265 Å, respectively,[22] in crystalline P_4Se_4 the mean P-Se and P-P bond lengths are 2.27 and 2.20 Å, respectively,[23] in crystalline P_4Se_3 the P-Se and P-P bond lengths are 2.24 and 2.25 Å, respectively,[24] and in crystalline white P the P-P bond length is 2.21 Å.[25] Because the real-space resolution may be estimated as $2\pi/Q_{\max} = 0.2$ Å in the glass diffraction measurements, the four types of nearest-neighbor correlations (including both P = Se and P-Se) cannot be clearly resolved. A special procedure was therefore adopted to obtain information about the separate correlations, making use of the information about the relative concentrations of the different structural units in Fig. 1 provided by the solid-state NMR experiments.[12]

In the Se-rich region, the Se-Se correlations were first separated out. Following the notation of Ref. 26, we define $N_a(b)$ to be the average number of neighbors of type b about an atom of type a, and $N_a = \sum_b N_a(b)$ to be the average number of atoms of all types about an atom of type a. Then the contribution of the pair (a,a) to the area of the first peak in the weighted average radial distribution function $rT(r)$ is given by $W_{aa}N_a(a)/c_a$, and that of the pair (a,b), $a \neq b$, by $2W_{ab}N_a(b)/c_b$, where the W_{ab} are the weighting factors defined in Eq. (3). The Se-Se coordination number at each composition was derived as follows. Clearly,

$$N_{\mathrm{Se}}(\mathrm{Se}) = N_{\mathrm{Se}} - N_{\mathrm{Se}}(\mathrm{P}) = N_{\mathrm{Se}} - \left(\frac{x}{1-x}\right) N_{\mathrm{P}}(\mathrm{Se}). \quad (4a)$$

Using the relations

$$N_{\mathrm{Se}} = 2 - \left(\frac{x}{1-x}\right) f_{\mathrm{P4}}, \quad (4b)$$

$$N_{\mathrm{P}}(\mathrm{Se}) = \frac{3}{2} f_{\mathrm{P1}} + 2 f_{\mathrm{P2}} + 3 f_{\mathrm{P3}} + 4 f_{\mathrm{P4}}, \quad (4c)$$

where the $f_{\mathrm{P}i}$ denote the relative frequencies the four structural units P1, . . . ,P4 shown in Fig. 1, we obtain

$$N_{\mathrm{Se}}(\mathrm{Se}) = 2 - \left(\frac{x}{1-x}\right)\left[\frac{3}{2} f_{\mathrm{P1}} + 2 f_{\mathrm{P2}} + 3 f_{\mathrm{P3}} + 5 f_{\mathrm{P4}}\right]. \quad (4d)$$

The relative frequencies $f_{\mathrm{P}i}$ for these units were taken from Ref. 12. Gaussian fits to the first peak in $T(r)$ were carried out at each composition, fixing the amplitude of the Gaussian corresponding to Se-Se correlations according to the values of $N_{\mathrm{Se}}(\mathrm{Se})$ derived from Eq. (4d), and allowing a free fit for a second Gaussian corresponding to both P-Se and P-P correlations. This second peak appeared at lower r as expected. A typical fit is shown in Fig. 4(b).

At low P concentrations, $x \leqslant 0.2$, the NMR results indicated a significant presence of $SePSe_{3/2}$ units with Se = P double bonds, which, according to the crystal data mentioned above, should be distinguishable from single P-Se and P-P bonds. Fits with three Gaussians were therefore carried out in this region. The amplitude of the second peak was fixed to meet the conditions

$$N_{\mathrm{P}}(\mathrm{Se})(\text{singly bonded}) = \tfrac{3}{2} f_{\mathrm{P1}} + 2 f_{\mathrm{P2}} + 3 f_{\mathrm{P3}}, \quad (5a)$$

$$N_{\mathrm{P}}(\mathrm{P}) = 3 f_{\mathrm{P0}} + \tfrac{3}{2} f_{\mathrm{P1}} + f_{\mathrm{P2}}, \quad (5b)$$

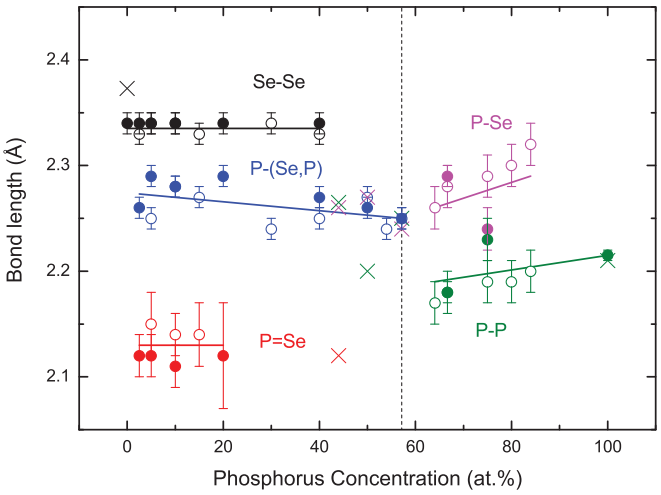

FIG. 5. (Color online) Bond lengths in P-Se glasses derived from the Gaussian fits; the points labeled P-(Se-P) represent the weighted average of single-bond P-Se and P-P correlations: neutron results, •; x-ray results, ○; crystal values, ×. The solid lines are a guide to the eye, and the dotted line indicates the P_4Se_3 composition.

and the amplitude of the Se-Se peak was kept fixed as before, allowing a free fit for a third Gaussian corresponding to P = Se correlations. A typical such fit is shown in Fig. 4(a).

In the P-rich region, Eq. (5b) was used to fix the amplitudes of the Gaussian corresponding to P-P correlations. Taking $f_{\mathrm{P2}} = 0$ in this region and neglecting the possibility of a small concentration of P_4Se_2 units suggested in Ref. 12, the frequencies are fixed by stoichiometry:

$$f_{\mathrm{P1}} = \frac{4(1-x)}{3x}, \quad f_{\mathrm{P0}} = 1 - f_{\mathrm{P1}}. \quad (6)$$

A second Gaussian corresponding to P-Se correlations was then fitted to $T(r)$. A typical result is shown in Fig. 4(c).

Results of the bond lengths and coordination numbers derived from these fits are shown in Figs. 5 and 6, respectively. Values from Se,[21] P,[25] and P_4Se_n (Refs. 6,7,22, and 23) crystals are shown for comparison.

IV. DISCUSSION

A. First sharp diffraction peak

FSDPs reflect the presence of local structural units in semiconducting glasses.[18,19] A model of random packing of structural units, based on a Percus-Yevick hard-sphere model for the arrangement of the centers of the units,[27,28] was found to reproduce the FSDP in P-Se glasses at $x = 0.4$ (Ref. 18) and $x = 0.5$ (Ref. 3) satisfactorily, although the structural unit chosen was the P_4Se_3 molecule rather than the $Se_{2/2}P\text{-}PSe_{2/2}$ units that, according to the NMR results, are the major component at these compositions, and, furthermore, the surrounding matrix was neglected.

In the Se-rich region, these considerations can be put on a more rigorous basis as follows. Suppose that the glass at a given composition x is composed of structural units with the formula P_mSe_{n-m} and volume V_p, embedded in a matrix of composition P_wSe_{1-w}. Clearly, $w \leqslant x \leqslant m/n$. Because the number density ρ_0 generally increases with x [Fig. 3(d)], we can write

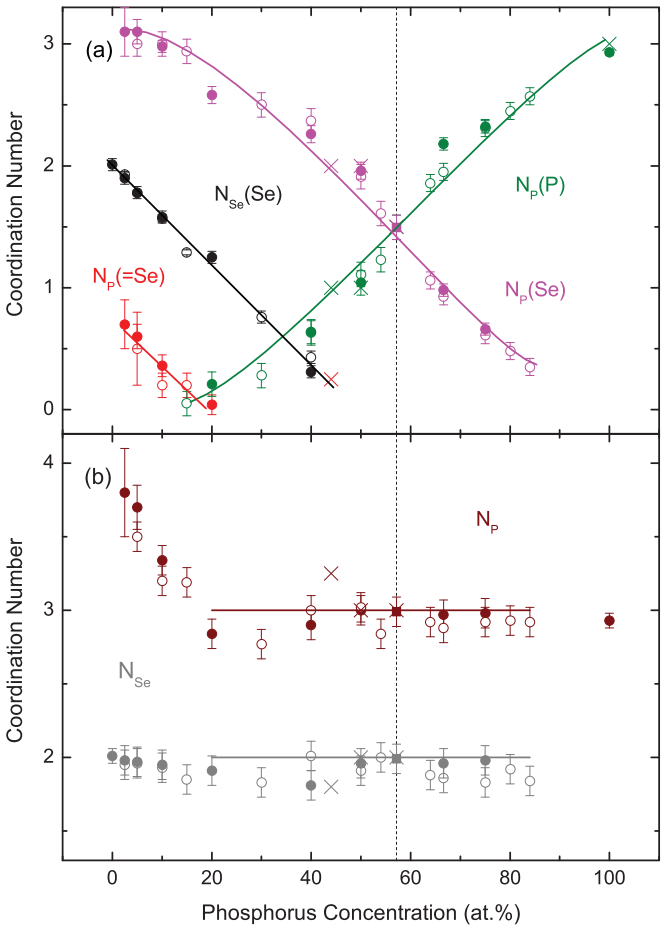

FIG. 6. (Color online) (a) Partial coordination numbers in P-Se glasses derived from the fitted Gaussians; (b) total coordination numbers for Se and P: neutron results, •; x-ray results, ○; crystal values, ×. The solid lines are a guide to the eye, and the dotted line indicates the P_4Se_3 composition.

$\rho(x) = (1+\alpha)^*\rho(w)$, where α is a small number that depends on w and x. It can be shown that

$$V_p = \frac{n}{\rho(w)\left(1+\frac{\alpha}{\eta}\right)}, \tag{7}$$

where η is the fraction of the volume filled by the structural units, and

$$x - w = \left(\frac{\eta-\alpha}{1-\eta}\right)\left(\frac{m}{n} - x\right). \tag{8}$$

Noting from Fig. 1, in conjunction with Fig. 8 of Ref. 12, that, as x increases, the predominant structural units have values of n equal to 3.5, 2.5, 4, and 7, Eq. (7) shows that V_p will generally increase with x approximately proportional to n, even though the mean atomic volume is decreasing [Fig. 3(d)]. If the volume V_p is approximated by a sphere of diameter σ, σ will increase as $n^{1/3}$. Calculations with the random packing of structural units model[29] mentioned above show that an increase in σ leads to both a shift of the FSDP to smaller Q and an increase in the amplitude, similar to the trend observed in Figs. 3(a) and 3(c). The increasing values of n will also lead to increase in the form factor of the unit at low Q, further enhancing these two effects. In the region at very low x, 0–0.05, where n decreases from 3.5 to 2.5, the very low values of the packing fraction η ($\sim x$) means that the structural units have very little contribution to the total structure factor.

Taking a numerical example at $x = 0.4$, where the principal structural unit is $Se_{2/2}P\text{-}PSe_{2/2}$ with $n = 4$, $m = 2$, and putting $\eta = 0.45$, the value used in the model calculation in Ref. 18, Eq. (8) gives $w \approx 0.32$, when $\rho(w) \approx 0.035\text{Å}^{-3}$, $\alpha \approx 0.035$, $V_p \approx 106$ Å^3, and $\sigma \approx (6V_p/\pi)^{1/3} = 5.9$ Å, reasonably close to the value 5.4 Å used in the model calculation that reproduces the FSDP.[18]

In the P-rich region, these trends are continued, with the FSDP increasing in amplitude and shifting to lower Q, but for a different reason. The FSDP in red amorphous P can be ascribed to a void structure,[30] in which in the voids are likely to be filled with an increasing concentration of P_4Se_3 units as the P concentration is reduced, resulting in a FSDP with lower amplitude and centered at higher Q. A similar trend is observed in applying pressure to red a-P.[30]

B. Feature in the structure factor at 7.5 Å^{-1}

In AIMD simulations of two P-Se glasses by Segri *et al.*,[5] this feature, which starts to appear at $x = 0.2$, shows up in a simulation of the glass at $x = 0.5$ started with intact P_4Se_3 molecules (five out of the original eight surviving) but not in one started from random atomic positions. Their two sets of results (fitted by a sixth-order polynomial) are compared with the present results at $x = 0.5$ in Fig. 7. The simulation starting with P_4Se_3 molecules gave excellent agreement for the position and width of the FSDP but the amplitude was lower, perhaps because P_4Se_3 is not the dominant unit at this composition.

C. Nearest-neighbor bond lengths and coordination numbers

Figures 5 and 6 show that a reliable interpretation of the diffraction data can be obtained with the information about the speciation obtained from the NMR results.[12] The bond lengths shown in Fig. 5 are consistent with the crystal data

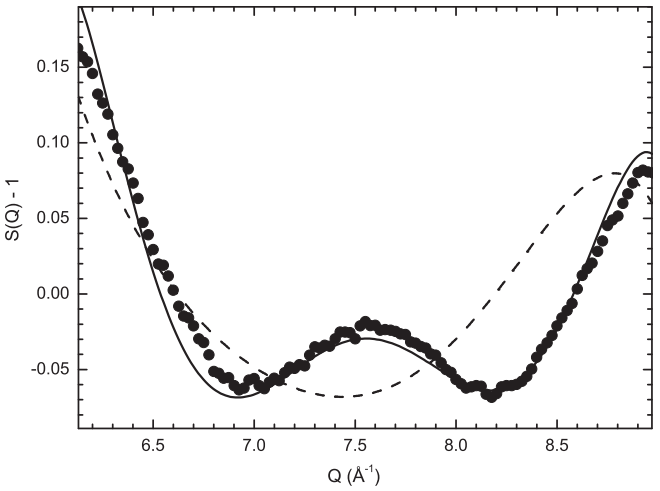

FIG. 7. Structure factor of PSe glass near $Q = 7.5$ Å^{-1}: points, neutron diffraction data; solid line, simulation of Sergi *et al.* (Ref. 5) started with intact P_4Se_3 molecules; dashed line, simulation started from random atomic positions.

referred to previously at compositions where these exist. In the Se-rich region the Se-Se and double P = Se bond lengths remain essentially constant, while the average of the P-P and single P-Se bond lengths shows a steady decrease by ∼1% as x increases from 0.025 to 0.54. Because the P-P bond length is slightly greater than the P-Se one in the crystals, this trend is probably owing to decreases in both P-Se and P-P bond lengths rather than the increasing weight of P-P bonds in the average. In the P-rich region the trend reverses, with both P-Se and P-P bond lengths increasing by ∼1% as x increases from 0.64 to 0.84.

The trends in speciation in the glasses are also generally similar to those observed in the crystals. A notable exception is the behavior of the double P = Se bonds, which are present in the crystal at $x = 4/9$ but not visible in the NMR data or the total correlation function beyond $x = 0.3$. Correspondingly, the P2 ($Se_{2/2}P\text{-}PSe_{2/2}$) species is predominant in the glasses for $x = 0.25$–0.5, but absent in the crystals.

In the total coordination numbers for P and Se shown in Fig. 6(b), it should be noted that the values of N_P are above 3 for $x = 0.025$–0.15 and those of N_{Se} below 2 for $x = 0.05$–0.3, both a consequence of the presence of P = Se bonds in this range.

V. CONCLUSIONS

This work has shown that not only can the previously contradictory NMR and diffraction results for the structure of P-Se glasses be reconciled, but also that, taken together, they lead to a comprehensive picture of the different structural units that evolve with a change in composition. As soon as small quantities, on the order of a few percent, of P are added to vitreous Se, structural units develop that lead to pronounced intermediate-range order on the length scale of ∼6 Å, as evidenced by the sharp FSDP at ∼1 $Å^{-1}$. Both the previous NMR[12] and the present diffraction data point to the presence of 4-coordinated P up to approximately $x = 0.3$, and the almost constant P = Se bond length in the region is quantified by the diffraction results. At approximately $x = 0.05$, 3-coordinated P becomes the dominant unit until approximately $x = 0.25$, where the ethylene-like $Se_{2/2}P\text{-}PSe_{2/2}$ units take over until the end of the Se-rich glass region at $x = 0.54$. A small concentration of P_4Se_3 molecularlike units starts to appear above $x = 0.3$ and increases up to the end of this region. The average of the irresolvable single P-Se and P-P bond lengths decreases slightly with increasing P concentration over this region, most likely owing to a simultaneous decrease in both bond lengths. Se-Se bonds, present up to approximately $x = 0.4$, have an almost constant length over this concentration range.

In the P-rich glass region that begins at $x = 0.64$ and continues up to pure red P, the concentrations of structural units in the NMR data were harder to quantify, but the dominant units were identified as P_4Se_3 and a red-P-like network, the latter dominating at the highest P concentrations. Neglecting the small concentrations of other units that could not be positively identified in the NMR, the relative concentrations of the two dominant units could be calculated. The peak intensities in the correlation functions derived from the diffraction data were consistent with these values. The P-Se and P-P bond lengths exhibited steady increases with increasing P concentration.

The apparent paradoxical behavior of the position in reciprocal space of the FSDP, decreasing with increasing P concentration in a similar way to the atomic volume, along with its steadily increasing intensity, can be explained in the Se-rich glass region by the increasing size of the units as the number of atoms they incorporate increases. In the P-rich region, on the other hand, this behavior can be explained by the void structure opening up as pure red P is approached.

The other intriguing feature in the diffraction pattern, the feature at 7.5 $Å^{-1}$ that starts to appear at $x = 0.4$, is further evidence of the presence of P_4Se_3 structural units at higher P concentrations.

ACKNOWLEDGMENTS

This work was supported by the CNRS and the Region Centre, France. The authors are grateful to the staffs at ISIS (Rutherford-Appleton Laboratory, UK), APS, ESRF, and SPring-8 for help with the experiments, and to F. Fayon (CEMHTI, Orléans) for helpful discussions. Work at the APS is supported by the US Department of Energy, Office of Science, Office of Basic Energy Sciences, under Contract No. DE-AC02-06CH11357.

*Present address: Institut Laue Langevin, 6 rue Jules Horowitz, BP 156, F-38042 Grenoble Cedex 9, France.

[1]Z. U. Borisova, *Glassy Semiconductors* (Plenum, New York, 1981), p. 70 (English translation).

[2]D. L. Price, M. Misawa, S. Susman, T. I. Morrison, G. K. Shenoy, and M. Grimsditch, J. Non-Cryst. Solids **66**, 443 (1984).

[3]M. Arai, R. W. Johnson, D. L. Price, S. Susman, M. Gay, and J. E. Enderby, J. Non-Cryst. Solids **83**, 80 (1986).

[4]G. M. S. Lister and R. Jones, J. Phys. Condens. Matter **1**, 6039 (1989).

[5]A. Sergi, M. Ferrario, F. Buda, and I. R. McDonald, Mol. Phys. **98**, 701 (2000).

[6]D. Lathrop and H. Eckert, J. Phys. Chem. **93**, 7895 (1989).

[7]D. Lathrop and H. Eckert, Phys. Rev. B **43**, 7279 (1991).

[8]D. G. Georgiev, M. Mitkova, P. Boolchand, G. Brunklaus, H. Eckert, and M. Micoulaut, Phys. Rev. B **64**, 134204 (2001).

[9]D. J. Verrall, L. F. Gladden, and S.R. Elliott, J. Non-Cryst. Solids **106**, 47 (1988).

[10]D. J. Verrall and S. R. Elliott, Phys. Rev. Lett. **61**, 974 (1988).

[11]R. T. Phillips, D. Wolverson, M. S. Burdis, and Y. Fang, Phys. Rev. Lett. **63**, 2574 (1989).

[12]A. Bytchkov, F. Fayon, D. Massiot, L. Hennet, and D. L. Price, Phys. Chem. Chem. Phys. **12**, 1535 (2010).

[13]C. J. Benmore and A. K. Soper, *A Guide to Performing Experiments on the Small Angle Neutron Diffractometer for Amorphous and Liquid Samples at ISIS*, version 1.0 (Rutherford-Appleton Laboratory Report, Didcot, UK, 1998).
[14]U. Rütt, J. R. Schneider, M. A. Beno, G. S. Knapp, and P. A. Montano, Proc. SPIE **3448**, 132 (1998).
[15]P. Suortti and T. Tschentscher, Rev. Sci. Instrum. **66**, 1798 (1995).
[16]S. Kohara, M. Itou, K. Suzuya, Y. Inamura, Y. Saukrai, Y. Ohishi, and M. Takata, J. Phys. Condens. Matter **19**, 506101 (2007).
[17]C. N. J. Wagner, J. Non-Cryst. Solids **179**, 84 (1994).
[18]S. C. Moss and D. L. Price, *Physics of Disordered Materials*, edited by D. Adler, H. Fritzsche, and S. R. Ovshinsky (Plenum, New York, 1985), pp. 77–95.
[19]D. L. Price, S. C. Moss, R. Reijers, M.-L. Saboungi, and S. Susman, J. Phys. Condens. Matter **1**, 1005 (1989).
[20]E. Lorch, J. Phys. C **2**, 229 (1969).
[21]P. Cherin and P. Unger, Inorg. Chem. **6**, 1589 (1967).
[22]G. T. Penney and G. M. Sheldrick, J. Chem. Soc. A **1971**, 245.
[23]M. Ruck, Z. Anorg. Allg. Chem. **620**, 1832 (1994).
[24]E. Keulen and A. Vos, Acta Crystallogr. **12**, 323 (1959).
[25]D. E. C. Corbridge and E. J. Lowe, Nature (London) **170**, 629 (1952).
[26]S. Susman, K. J. Volin, D. L. Montague and D. L. Price, J. Non-Cryst. Solids **125**, 168 (1990).
[27]M. F. Daniel, A. J. Leadbetter, A. C. Wright, and R. N. Sinclair, J. Non-Cryst. Solids **32**, 271 (1979).
[28]N. W. Ashcroft and J. Lekner, Phys. Rev. **145**, 83 (1966).
[29]D. L. Price (unpublished).
[30]J. M. Zaug, A. K. Soper, and S. M. Clark, Nat. Mater. **7**, 890 (2008).